Research Report
2004-07

Reduced Cost Current-Source Topology Improving the Harmonic Spectrum Through On-Line Functional Minimization

Tenca, P., T.A. Lipo
Email: tenca@cae.wisc.edu, lipo@engr.wisc.edu

Dept. of Elect. & Comp. Engr.
University of Wisconsin-Madison
1415 Engineering Drive
Madison, WI 53706

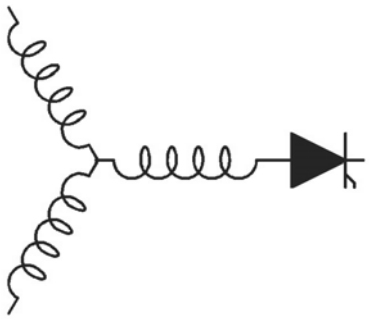

Wisconsin
Electric
Machines &
Power
Electronics
Consortium

University of Wisconsin-Madison
College of Engineering
Wisconsin Power Electronics Research Center
2559D Engineering Hall
1415 Engineering Drive
Madison WI 53706-1691

Reduced cost Current-source Topology improving the Harmonic Spectrum Through On-line Functional Minimization

Pierluigi Tenca
University of Wisconsin-Madison
Engineering Hall, 1415 Engineering Drive
Madison, WI, 53706 U.S.A.
Email: tenca@cae.wisc.edu

Thomas A. Lipo
University of Wisconsin-Madison
Engineering Hall, 1415 Engineering Drive
Madison, WI, 53706 U.S.A.
Email: lipo@engr.wisc.edu

***Abstract*—The paper presents a Current-Source Inverter (CSI) topology tailored for large multi-megawatt wind turbine applications. The cable distance between the generator and the mains enables the realization of a significant portion of the DC-link inductance. In order to improve the efficiency and to allow the possible utilization of rugged inexpensive Thyristors, PWM modulation is not used in the main conversion chain. Unity fundamental power factor at the mains is guaranteed at any load condition while the 5^{th} and 7^{th} harmonics of the mains line currents are reduced by choosing a proper nominal operating point for the turbine. Further harmonic reduction is achieved through an active filter controlled via a newly proposed methodology suitable for Digital Signal Processor (DSP) implementation. Such a controller relies on a real-time minimization of a proper functional and is capable of implementing true-feedback current regulation. A part of design simulation results, aimed at constructing a 10 kW prototype, are presented.**

I. INTRODUCTION

Large multi-megawatt wind turbines will be more and more pervasive in the next future bringing stringent requirements to their energy conversion processes as well as on their operational costs. Reduced construction and life-cycle costs, low harmonic content in the line currents delivered to the mains, high-efficiency and reliability are all factors of prominent importance for such systems.

The paper proposes a topological solution suitable to satisfy these requirements and based on a Current-Source Inverter (CSI) concept. The nature of the CSI topologies takes advantage of the inductance contribution present in the loop constituting the DC-link. As consequence this solution exploits the distance between the generator and the mains characterizing the wind turbines to realize a significant portion of the DC-link inductance.

In order to improve the efficiency and to allow the utilization of rugged inexpensive semiconductors (Thyristors), the proposed solution avoids PWM modulation in the "Main Conversion Chain" (MCC). This solution adopts reduced cost topological sub-systems devoted to convert the total average power caught from the wind.

Other authors [1] have proposed a CSI topology based on a single phase-angle controlled thyristor bridge but such a solution requires compensating also the reactive power generated by the bridge in order to increase the fundamental power factor at the mains. As consequence the active compensator needs to be designed for significant current ratings and, in case of its failure, no possible alternative would exist to compensate the reactive power.

Conversely, the topological solution proposed here relies on two CSI bridges connected in series. Both are still controlled via the well-established phase-angle control technique but using exactly opposite control angles. This choice, together with other features, guarantees unity modulus of the fundamental power factor at all operating points of the turbine. Furthermore, proper design choices reduce the 5^{th} and 7^{th} harmonic of the mains line currents at the nominal operating point of the turbine simply using the MCC only.

The use of an active filter leads to further harmonic reduction in the line currents but, differently from the solution proposed in [1], it does not need to compensate for the reactive power at mains frequency. Failure of the filter does not prevent a-priori the system from operating at full power and from guaranteeing unity fundamental power factor, since this feature is intrinsic in the MCC itself.

The control methodology used for the active filter relies on a newly proposed technique whose basis has been introduced by the authors in [7]. The controller relies on the real-time minimization of a proper time-varying functional, whose analytical limit for $t \to +\infty$ equals the average power of the current error as defined in traditional signal theory.

The methodology realizes true feedback in the current synthesis process, without any need to rely on off-line, open-loop, computations or on a-priori assumed waveforms. This is a key and distinctive feature when compared to different established solutions proposed by other authors in the past.

II. OVERVIEW OF THE PROBLEM

The converters present in the several existing wind turbines are usually based on classical Voltage Source Inverter (VSI) topologies and radial-flux generators. In many state-of-the-art wind turbines the generator and the needed VSI converters are located in the nacelle at the top of the tower leaving only the Mains interconnection transformer at the ground level [2], [3], [5], [6].

A non-negligible reason for this arrangement lies in the need to minimize these stray inductances that would be

otherwise harmful to the proper operation of the VSI type conversion chain. Such an arrangement renders the wind turbine expensive and difficult to maintain because several bulky and reliability-critical components (especially the DC-link capacitors) are required.

Furthermore in order to meet the power quality standards (such as IEEE 519-1992) significant PWM modulation [2], [3] is used in the main conversion chain which is often rated for the totality of the generated power. This reduces the efficiency, mainly because of the switching losses, and enhances the stresses on the main switches ultimately increasing their likelihood of failure and the system life cycle-costs. The rapidly growing power ratings of the wind turbines simply aggravate these drawbacks.

III. Proposed Topological Solution

The authors propose in this paper an alternative current-source topology shown in Figure 1 where the square boxes identify topological structures organized as the common three-phase bridges. The topology is based on a current-source concept [8], [9] whose intrinsic nature takes advantage of the distance between the generator and the mains and this feature is exploited indeed to realize a major portion of the needed DC-link inductance.

Only two power cables are needed between the nacelle and ground and only a very reliable switch module (diode bridge A) is located at the top of the tower thereby reducing the weight of the nacelle and the overall maintenance costs.

The total average power is converted by the two series-connected current-source inverters (B and C) independently supplied by the two equal secondaries of a Y-Y-Delta transformer. They are part of the Main Conversion Chain (MCC) (drawn with gray background in Figure 1) and are controlled by the well-known phase-control technique [8], [9] whose switching frequency equals the mains frequency (no PWM) thereby minimizing the switching losses.

The key point of the control is to operate the two inverters with opposite phase-control angles so that the fundamental power factor of the mains line currents at the transformer primary is guaranteed to be unity at any load condition. As consequence of this choice one of the two inverters must use fully controllable switches with bi-directional voltage blocking capability. Despite this necessity, and thanks to the absence of any PWM modulation, the use of inexpensive standard thyristors could be potentially possible in both inverters provided that well-known auxiliary commutation circuits were used in the bridge C (ASCI inverter for example).

This reduces significantly the cost of the topology, renders it suitable for very high power wind turbines and improves its reliability due to the well known ruggedness characterizing the use of thyristors.

IV. Design of the Main Conversion Chain

This section describes the peculiar design choices concerning the MCC leading to an improved spectrum of the mains line currents.

In the following K_thyr and K_fc are defined as the ratios between the phase secondary voltage and primary line-to-line voltage for the secondaries connected to the thyristors and fully controllable inverter respectively. The phase-control angle $\varphi \in [0, \pi)$ [rad] is defined for the thyristor inverter according to the commonly used conventions [8], [9]. Idc represents the DC-link current assumed ideally constant and $n \in Z$ is the harmonic order of the n-th spectral component in the bilateral Fourier spectrum.

It can be proven straightforwardly that the complex Fourier coefficient C_Im(n) associated with the n-th spectral component of the phase a mains line current has the form shown in Equation (1).

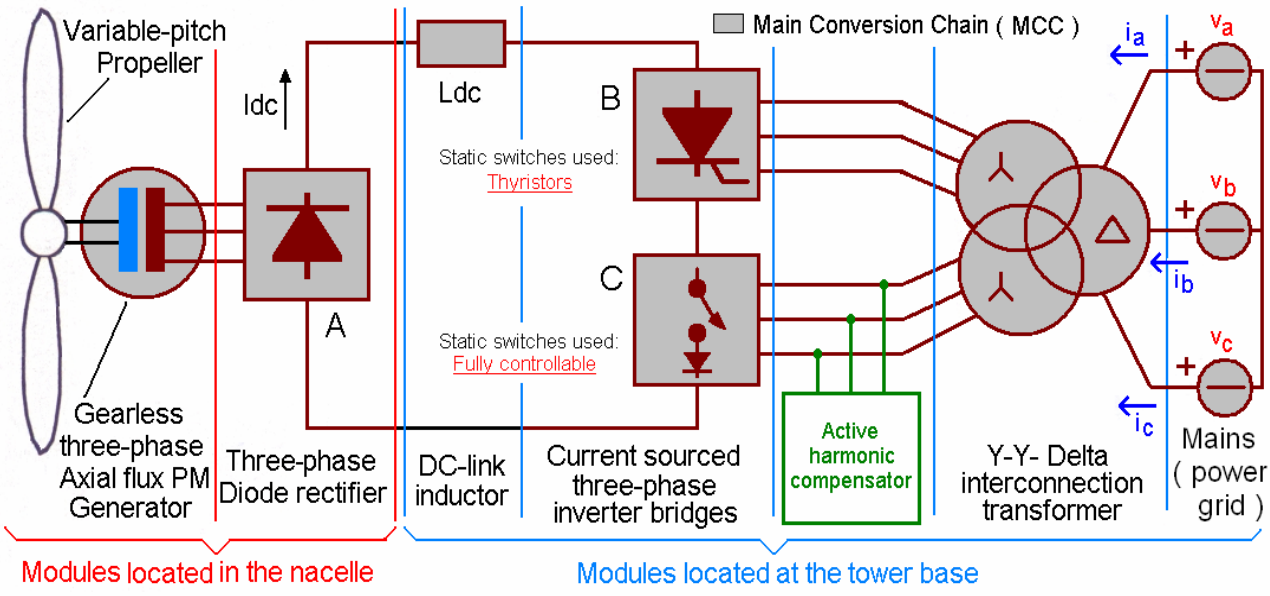

Fig. 1 Concept of the proposed topology

$$C\_Im(n) = Idc \cdot \cos\left(\frac{n\pi}{6}\right) \cdot \frac{A(n)}{n\pi} \cdot B(n, \varphi, K\_thyr, K\_fc)$$

where $n \in Z - \{0\}$ and:

$$A(n) = \left[1 - \cos\left(\frac{4n\pi}{3}\right) + j \cdot \sin\left(\frac{4n\pi}{3}\right)\right] \cdot \left[-1 + (-1)^n\right] \quad (1)$$

$$B(n, \varphi, K\_thyr, K\_fc) = j \cdot \left[K\_thyr \cdot e^{j \cdot (n\varphi)} + K\_fc \cdot e^{-j \cdot (n\varphi)}\right]$$

Figure 2 shows the ratios $2 \cdot |\, C\_Im(n) \,| \,/\, Idc$ computed from Equation (1) for n = {5,7}, equal transformer secondaries characterized by K_thyr = K_fc = 1/sqrt(3) and φ in the interval [π/2, π) where both bridges operate as inverters.

The analysis of Equation (1) reveals that the three values of the control angle φ listed in Table I already reduce the harmonic content of the mains line current without need for PWM action. In particular the angle φ3 reduces the total average power contained in the 5th and 7th harmonic and allows a good utilization factor of the two bridges.

It should be observed that the pitch control of the propeller blades usually keeps the generator at its nominal rotational speed [6] in a suitable range of wind speeds.

TABLE I

VALUES OF THE PHASE-CONTROL ANGLE φ REDUCING THE HARMONIC CONTENT OF THE MAINS LINE CURRENT

$\varphi 1 = (9/10)\pi$	Nullifies the 5th harmonic
$\varphi 2 = (13/14)\pi$	Nullifies the 7th harmonic
$\varphi 3 = 0.914\,\pi$	Minimizes the total average power in the 5th and 7th harmonics

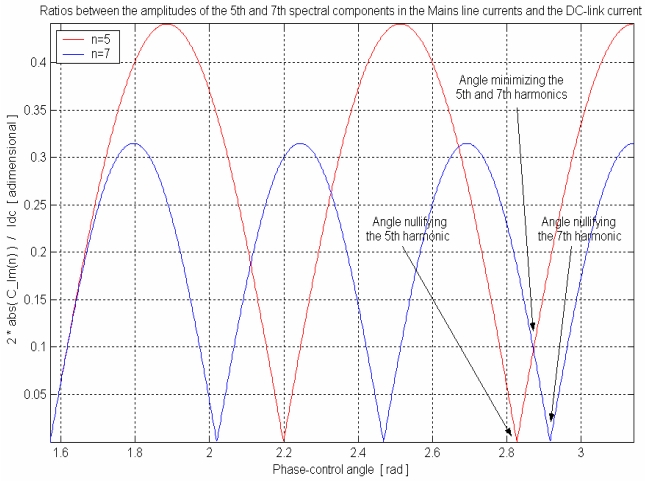

Fig. 2 Ratios between the amplitudes of the 5th and 7th spectral components in the mains line currents and DC-link current

This suggests that one must design the generator with as low stray inductance and resistance as possible. In this manner the output voltage undergoes reduced dependence from the output current and it is maintained close to its nominal value by the indirect action of the pitch controller. A specially designed axial-flux permanent magnet generator has been chosen as suitable solution capable to satisfy such a requirement.

The additional key design choice concerning the generator is the value of its nominal voltage. This value is chosen in such a way that the DC-link controller is forced to issue the values ±φ3 of the control angles to the bridges B and C at nominal mains voltage. In this manner the 5th and 7th harmonics in the line currents are intrinsically reduced as explained previously. In general any specific component of the MCC must be designed for the nominal operating point characterized by the values of the electrical quantities associated with the control angle φ3.

The DC-link current is regulated by means of variations of the phase-control angle φ. In the steady state such variations are small and occur around the nominal value φ3. The DC-link current controller can be implemented very simply and cost-effectively by using a suitable PI regulator whose input is the error between the desired and actual DC-link current. Additionally, several PI regulators are available off-the shelf in the market helping to reduce the design costs.

It is worthwhile to mention that only one current sensor located at the base of the tower may suffice, avoiding the need for additional sensors in the nacelle. Nevertheless the possible use of a sensor measuring the voltage directly at the output of the diode bridge (A), might certainly improve the dynamic of the DC-link current, provided that a more complex controller is used.

The proposed topology has been fully modeled in Simplorer / Simulink also with the goal to define the design of a 10 kW prototype currently under construction. The following figures show some of the design simulations results aimed at illustrating the behavior of the converter. The most important parameters concerning the MCC are: Ldc = 100 mH, mains line-to-line voltage = 460 V, transformer secondary line-to-line voltage = 460 V, nominal Idc = 10 A and peak voltage of the generator phase back-emf = 644 V.

Figure 3 shows that the regulator at steady state maintains φ in the neighborhood of φ3 (~ 165 degrees) when the properly designed generator operates at its nominal point. Figure 4, in the interval [0.22 , 0.25] [s], shows the line currents (blue) when φ and Idc are close to φ3 and 12.5 A respectively.

The undesired harmonics are further reduced through an active harmonic compensator constituted by a VSI connected to the same secondary of the bridge C via series inductances of proper value. This VSI (drawn in green in Figure 1) is not part of the MCC and it does not deliver any active or reactive power at mains frequency. The active harmonic compensator uses fully controllable switches

operating at frequency much higher than the mains frequency. These switches normally undergo higher dynamic stresses than those used in the MCC and belong to a type (usually an IGBT) less reliable than the Thyristor. Hence the active harmonic compensator is the sub-system most prone to fail. However, the proposed solution avoids the possible complete loss which might impair the main functionality of the wind turbine. If the active harmonic compensator fails, it can be completely disconnected from the MCC leaving it capable of operating at full power, with unity fundamental power factor and with reduced 5th and 7th mains line current harmonics. Obviously in this emergency case the spectrum of the mains line current is degraded.

A properly connected diode rectifier allows the DC-link capacitor of the VSI harmonic compensator to act as snubber for the bridge C that does not commutate naturally while B does. This is the reason why the active harmonic compensator has been connected to the output of bridge C instead of B. In this manner the energy otherwise lost in other possible snubbing solutions is used to help charging the DC-link capacitor.

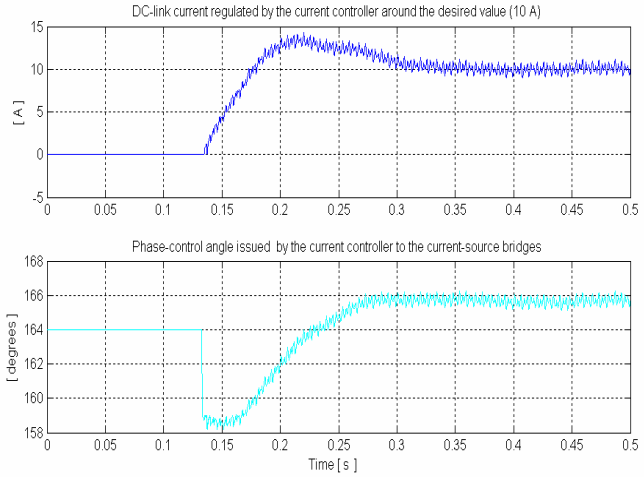

Fig. 3 Regulation of the current Idc and phase-control angle φ as performed by the DC-link current controller

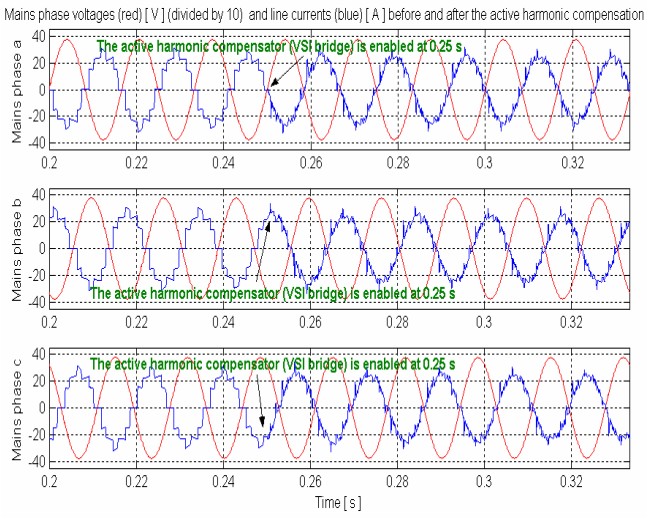

Fig. 4 Mains line currents (blue) before and after the VSI active harmonic compensator is enabled at the instant 0.25 s.

V. Principles of the Variational Controller

The control technique used for the active harmonic compensator belongs to the normal PWM class of controllers but the switching instants and sequence of switching states for the VSI are determined by a carrierless approach based on the real-time minimization of the time-varying real functional $\Psi(t)$ defined in $\Re^+$ and shown in Equation (2). $\Psi(t)$ is constituted by the sum of 3 positive-definite functions of time $\Psi_\gamma(t)$, one for each mains phase. The three mains phases are identified by the letters {a,b,c} represented symbolically by the subscript variable γ. The functions $i_\gamma(t)$ and $i_{\gamma\_ref}(t)$ constitute the actual and reference line currents of the active harmonic compensator respectively.

$$\psi(t) = \sum_{\gamma=\{a,b,c\}} \underbrace{\frac{1}{t}\cdot\int_0^t \left[i_\gamma(\tau) - i_{\gamma\_ref}(\tau)\right]^2 d\tau}_{\psi_\gamma(t) \text{ and } t\in(0,+\infty)} \qquad (2)$$

Under the hypothesis that each line current is a bounded and alternating signal with period T, it can be observed straightforwardly that the limit of $\Psi_\gamma(t)$, $\gamma=\{a,b,c\}$ for $t \to +\infty$ is finite and equal to the definite integral written at the right-hand side (RHS) of Equation (3).

$$\lim_{t\to+\infty} \underbrace{\frac{1}{t}\cdot\int_0^t \left[i_\gamma(\tau) - i_{\gamma\_ref}(\tau)\right]^2 d\tau}_{\psi_\gamma(t) \text{ where } \gamma=\{a,b,c\}} = \frac{1}{T}\cdot\int_0^T \left[i_\gamma(\tau) - i_{\gamma\_ref}(\tau)\right]^2 d\tau \qquad (3)$$

Such definite integral constitutes the average power of the periodic "error" signal $i_\gamma(t)$ - $i_{\gamma\_ref}(t)$ as defined by the signal theory [10], [11], [12] and it can be expressed in the frequency domain via the Parseval's identity. Therefore Equation (3) can be rewritten as Equation (4), where $\alpha_{I\gamma}(n)$ and $\alpha_{I\gamma\_ref}(n)$ are the n-th bilateral Fourier spectral components of $i_\gamma(t)$ and $i_{\gamma\_ref}(t)$ respectively.

$$\lim_{t\to+\infty} \psi_\gamma(t) = \sum_{n=-\infty}^{+\infty} \left|\alpha_{I\gamma}(n) - \alpha_{I\gamma\_ref}(n)\right|^2 \quad \text{where} \quad \gamma=\{a,b,c\} \qquad (4)$$

The RHS of Equation (4) can be interpreted also as the squared "distance" [15] – in the sense of the Euclidean norm - between the two infinite dimensional vectors whose elements are $\alpha_{I\gamma}(n)$ and $\alpha_{I\gamma\_ref}(n)$. The synthesis of the line currents $i_\gamma(t)$ capable of minimizing the average power

expressed by the RHS of Equation (3) can be seen as a problem of calculus of variations with moving boundaries [14], as the authors highlighted in a previous paper [7].

The controller builds in real-time the sequence of switching states generating the currents $i_\gamma(t)$ capable to make $\Psi(t)$ converge towards its absolute minimum (i.e. 0). Consequently, because of Equation (3), the controller minimizes asymptotically the functional comprised of the average power, thus solving in real-time the aforementioned variational problem.

Such a vision of the line currents synthesis justifies the name "variational controller" assigned to this technique by the authors. Furthermore it can be proven easily [7] that when the reference signals $i_{\gamma\_ref}(t)$ are sinusoidal, this control technique minimizes the Total Harmonic Distorsion (THD) factor of the synthesized line currents $i_\gamma(t)$.

VI. True feedback algorithm used to implement the variational controller

The proposed controller operates on a discrete-time basis, ruled by a proper clock signals having constant frequency $f_c = 1/T_c$ selected to be suitably higher than the fundamental frequency of $i_{\gamma\_ref}(t)$. At each clock event the controller computes the total time-derivative of $\Psi(t)$ - shown in Equation (5) - for each one of the 8 switching states allowed for the VSI. The switching state minimizing $d\Psi(t)/dt$ is selected as "optimal" for the current clock period and kept unchanged for the next T_c seconds.

$$\frac{d\,\psi(t)}{d\,t} = \sum_{\gamma=\{a,b,c\}} \left\{ \begin{array}{c} \overbrace{-\frac{\psi_\gamma(t)}{t}}^{\text{term A}} + \\ + \underbrace{\frac{\overbrace{\left[i_\gamma(t) - i_{\gamma\_ref}(t)\right]^2}^{Esq_\gamma(t)}}{t}}_{\text{term B}} \end{array} \right\} \qquad (5)$$

This switching state is defined as "optimal" because when the associated minimum of $d\Psi(t)/dt$ is negative, such state contributes to drive the functional $\Psi(t)$ towards its absolute minimum with the greatest effectiveness possible. As the time progresses the sequence of "optimal" switching states is generated in real-time according to this selection criterion applied at each clock event.

When the overall operating conditions of the converter allow that sequence to render negative the average of the minima assumed by $d\Psi(t)/dt$, then $\Psi(t)$ converges to its absolute minimum asymptotically. Consequently, because of Equations (3), the actual currents $i_\gamma(t)$ synthesized by the generated sequence of "optimal" switching states constitute the solutions (extremals) of the variational problems and ultimately track the references $i_{\gamma\_ref}(t)$, $\gamma=\{a,b,c\}$ as desired.

The system dynamics must be necessarily included in the computation of $d\Psi(t)/dt$. Indeed any switching state influences directly and only the VSI phase voltages via algebraic expressions reflecting the topological structure associated with such state. Conversely, because of the inductances in series to the VSI phases, the actual line currents derive from at least one level of time-integration performed on expressions involving those voltages. As consequence, a switching state selected at a specific clock instant t_c can influence the line currents only for $t > t_c$.

In order to consider this dynamics Equation (5) is expanded in the form of Equation (6) where the squared current error $Esq_\gamma(t)$ is defined by the brackets present in Equation (5). As explained previously, the controller calculates $d\Psi(t)/dt$ via Equation (6) at the instant t_c triggered by a new clock event but, conceptually, this computed value of $d\Psi(t)/dt$ belongs to the NEXT clock instant t_c+T_c.

$$\left.\frac{d\,\psi(t)}{d\,t}\right|_{t = t_c + T_c} = \sum_{\gamma=\{a,b,c\}} \left[\begin{array}{l} \overbrace{\left\{ \begin{array}{l} -\frac{t_c}{(t_c+T_c)^2}\cdot\psi_\gamma(t_c) + \\ \overbrace{\int_{t_c}^{t_c+T_c}\left[i_{\gamma\_m}(\tau) - i_{\gamma\_m\_ref}(\tau)\right]^2 d\tau}^{C_\gamma(t_c,T_c)} \\ -\frac{t_c}{(t_c+T_c)^2} + \\ +\frac{Esq_\gamma(t_c+T_c)}{(t_c+T_c)} \end{array} \right\}}^{\text{term A}} \text{term B} \end{array} \right] \qquad (6)$$

The need for an estimate of the actual line currents in the inteval (t_c , t_c+T_c] clearly arises from the observation of the terms $C_\gamma(t_c , T_c)$ and $Esq_\gamma(t_c+T_c)$ in Equation (6). The controller generates this estimate by computing numerically the known analytical solution of the proper differential equations describing the system dynamics. In addition to knowledge of the series inductances, this computation involves the values of the line currents $i_\gamma(t)$ and secondary transformer voltages, both measured at t_c and assumed constant in the interval (t_c , t_c+T_c].

The previous description and reasoning evidence the key features of the proposed control method: a) The absence of any carrier and/or a-priori chosen waveform. b) The implementation of the control action completely in real-time without any a-priori needed off-line pre-computation. c) The controller performs a true feedback current synthesis, because at any clock event it measures the state variables of the network and uses their values in the computation of $d\Psi(t)/dt$.

The derivative $d\Psi(t)/dt$ is the only quantity on which the selection of the switching states relies and it is worthwhile to highlight that its analytical expression is known. This allows its direct computation avoiding the need of

estimating it numerically from the knowledge of $\Psi(t)$. Such a procedure indeed would be always highly inaccurate, when not totally unfeasible.

By increasing the controller clock frequency a less accurate estimate would be possible and vice versa. The authors believe that it is important to investigate properly the optimum balance between clock frequency and accuracy of the estimate in any specific application of this control method. Both means improve the controller performance but they are linked to different practical drawbacks. On one hand higher clock frequency demands for faster switches and DSP processors while leading also to higher switching losses. On the other hand a better estimate requires more precise knowledge of the system parameters (e.g. line inductances of the harmonic compensator) which is difficult to obtain in certain applications.

VII. Variational Controller Applied to the Active Harmonic Compensator

Before applying the previously illustrated control technique to the active harmonic compensator used in the proposed topology it is necessary to determine the reference currents $i_{\gamma\_ref}(t)$, $\gamma=\{a,b,c\}$ constituting one of the controller inputs. In this case the currents $i_{\gamma\_ref}(t)$ have fundamental frequency higher than the mains frequency because the harmonic compensator does not deliver any reactive power at mains frequency. Furthermore, the waveforms of $i_{\gamma\_ref}(t)$ have discontinuous first-order time derivative and, in some time intervals, such derivative assumes very high values (steep slopes characterize these waveforms). This occurs because $i_{\gamma\_ref}(t)$ must compensate the fast transitions present in the line currents at the output of the two CSI inverters B and C in the MCC.

By measuring the mains line currents and phase voltages at the transformer primary it is possible to compute the average power delivered to the mains which is clearly unaffected by the corrective action of the harmonic compensator. Hence it is straightforward to compute the purely sinusoidal mains line current $i_{a\_sin}(t)$, $i_{b\_sin}(t)$, $i_{c\_sin}(t)$ that would deliver the same average power while having the desired phase displacement with respect to the mains phase voltages. In this case π [rad] is desired according to the conventional reference directions depicted in Figure 1.

The last step involves the knowledge of the transformer structure, its transformation ratios and the measured currents at the output of the bridges B and C. From this information it is finally possible to derive indirectly, via simple algebraic relationships, which are the corrective currents $i_{\gamma\_ref}(t)$ that the harmonic compensator must synthesize to obtain $i_{a\_sin}(t)$, $i_{b\_sin}(t)$, $i_{c\_sin}(t)$ at the mains.

The following figures show some of the simulation results aimed at designing the 10 kW prototype for which the use of Texas Instruments TMS320F240 DSP processors is planned. The results are obtained with 750 V DC-link voltage, 10mH line inductance and 10 kHz clock frequency (i.e. f_c). The improved mains line currents waveforms consequent to the action of the active harmonic compensator under variational control are shown in Figure 4 after 0.25 s. Figure 5 shows again, with better detail, the corrected mains line currents (blue) together with their sinusoidal references $i_{a\_sin}(t)$, $i_{b\_sin}(t)$, $i_{c\_sin}(t)$ (magenta) computed inside the controller as explained previously.

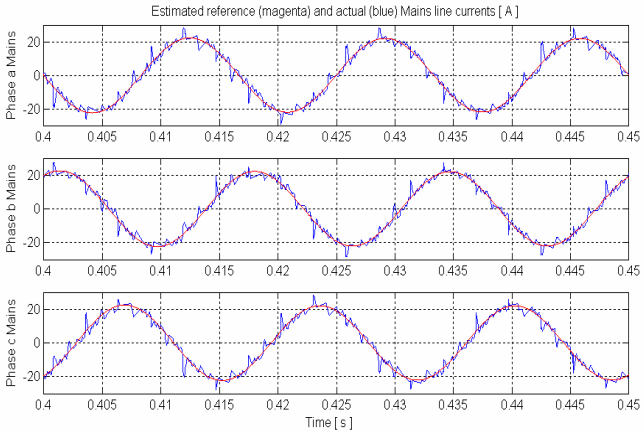

Fig. 5 Reference (magenta) and actual (blue) mains line currents

Figure 6 shows the monolateral amplitude spectrum of the line current flowing in the mains phase a up to 2 kHz. The upper graph (blue) shows the harmonic amplitudes together with information about the fundamental and its phase displacement with respect to the related mains phase voltage. The lower graph (red) shows the harmonic amplitudes expressed in percent of the fundamental. It is possible to observe that the 13th harmonic (780 Hz) is about 5% of the fundamental while the 11th (660 Hz), 7th (420 Hz), 5th (300 Hz) are below 4%, 3% and 1.5% respectively .

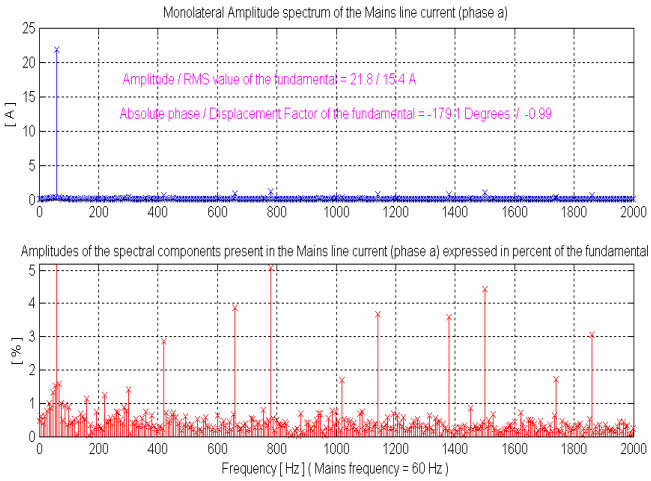

Fig. 6 Spectrum of the corrected mains line currents

Figure 7 shows the reference currents (magenta) $i_{\gamma\_ref}(t)$, $\gamma=\{a,b,c\}$ for the active harmonic compensator, computed as explained previously, together with the actually synthesized line currents (blue).

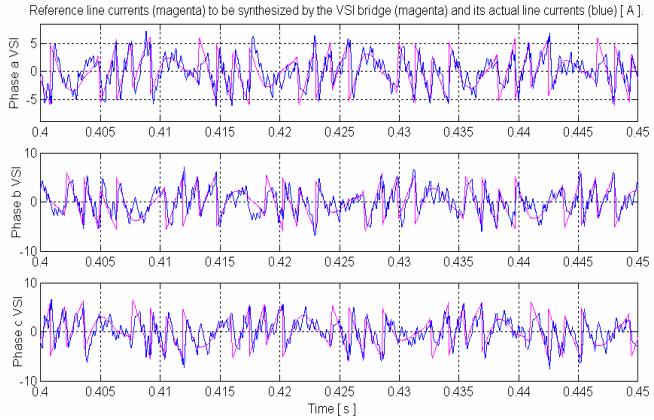

Fig. 7 Reference (magenta) and synthesized (blue) line currents for the active harmonic compensator

The almost vertical slopes characterizing $i_{\gamma\_ref}(t)$ in some intervals of time can be easily observed in Figure 7. In practice the rate of rise and rate of fall of the synthesized currents is always limited by the available DC-link voltage. This leads sometimes to significant local deviations from the desired $i_{\gamma\_ref}(t)$ in those intervals as is clearly observable in Figure 7. Such deviations are responsible for the short peaks with high-frequency content observable in the mains line currents (blue) shown in Figure 5. These peaks may certainly be reduced by designing higher current derivatives until reasonable practical limits are reached, but they cannot be completely eliminated. Hence, from the practical point of view, it is always advisable to provide a small-size high-frequency passive filter at the mains terminal to deal with high-frequency side effects such as these.

Figure 8 shows the functional $\Psi(t)$ (blue) decreasing under the action of the variational controller which renders $d\Psi(t) / dt < 0$ (red) for most part of the time. The functional $\Psi(t)$ is recorded at each simulation step while $d\Psi(t)/dt$ is computed only on a discrete-time basis, every T_c seconds, when a clock event triggers a new quest for the next optimal switching state.

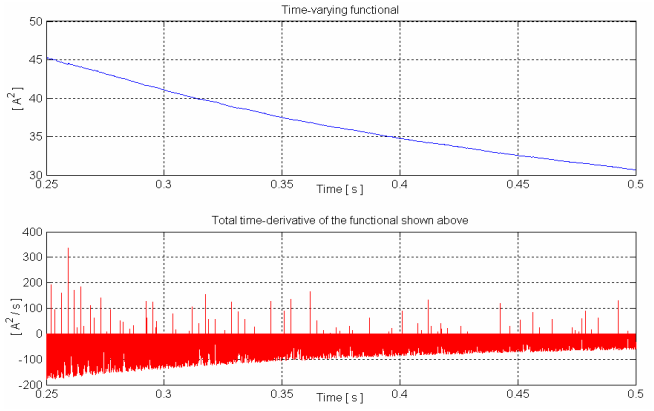

Fig. 8 $\Psi(t)$ (blue) and $d\Psi(t) / dt$ (red) computed every T_c [s]

Some applications of this control method where a complex dynamics is involved might require for very fast DSPs or FPGAs. This might constitute a drawback of the method at the present time but it must be realized that processors speed increases steadily, rendering such potential limit more and more negligible as the time elapses. This paper suggests a methodological approach conceived not only for the present but also projected to future potential applications involving voltage link as well as current link PWM converters.

VIII. CONCLUSION

A cost-effective and rugged conversion topology conceived for the emerging high-power wind turbines has been presented. The proposed topology is based on a CSI concept that exploits the intrinsic distance between the generator and the mains peculiar of the wind turbines. The proposed solution does not use PWM modulation in the conversion of the average power allowing the use of inexpensive and rugged Thyristors. At the same time, it guarantees unitary fundamental power factor and somehow reduced harmonic content already without filtering action. Further harmonic reduction is provided by an active harmonic compensator whose possible failure does not impede the full power operation of the turbine. The active harmonic compensator is controlled via a newly proposed carrierless variational method capable of real-time, true feedback, operation.

REFERENCES

[1] Z. Chen, E. Spooner, "Current source thyristor inverter and its active compensation system", *IEE Proceedings Generation Transmission and Distribution*. Vol. 150 No. 4 July 2003.

[2] A.M. El-Tamaly, H.H. El-Tamaly, E. Cengelci, P.N. Enjeti, E. Muljadi: "Low cost PWM converter for utility interface of variable speed wind turbine generators", *Applied Power Electronics Conference and Exposition, 1999. APEC '99*. Fourteenth Annual, Volume 2, 14-18 March 1999, Page(s): 889 –895.

[3] R. Pena, J.C. Clare, G.M. Asher: "A doubly fed induction generator using back-to-back PWM converters supplying an isolated load from a variable speed wind turbine", *Electric Power Applications, IEE Proceedings,* Volume: 143 Issue: 5, Sept. 1996, Page(s): 380 –387.

[4] G. Poddar, A. Joseph, A.K. Unnikrishnan: "Sensorless variable-speed controller for existing fixed-speed wind power generator with unity-power-factor operation", *IEEE Transactions on Industrial Electronics,*, Volume: 50 Issue: 5, Oct. 2003, Page(s): 1007 –1015.

[5] C.L. Kana, M. Thamodharan, A. Wolf: "System management of a wind-energy converter", *IEEE Transactions on Power Electronics,* Volume: 16 Issue: 3, May 2001, Page(s): 375 –381.

[6] E. Muljadi, C.P. Butterfield: "Pitch-controlled variable-speed wind turbine generation", *IEEE Transactions on Industry Applications*, Volume: 37 Issue: 1, Jan.-Feb. 2001, Page(s): 240 –246.

[7] P. Tenca, T.A. Lipo: "Synthesis of Desired AC Line Currents in Current-sourced DC-AC Converters", *IEE Power Electronics Machines and Drives 2004*, *PEMD '04*, Volume 2, Page(s): 656-661, Edinburgh, 31 March – 2 April 2004.

[8] P. Wood: *Switching Power Converters*. (book) Van Nostrand Reinhold Company, 1981.

[9] B.R. Pelly: *Thyristor Phase-Controlled Converters and Cycloconverters.* (book) Wiley-Interscience, 1971.

[10] A. Papoulis: *The Fourier Integral and its Applications*. (book) Mc Graw-Hill Book Company, 1962.

[11] S.I. Baskakov: *Signals and Circuits.* (book) MIR publisher Moscow, 1986.

[12] A. Papoulis: *Signal Analysis.* (book) Mc Graw-Hill Book Company, 1984.

[13] H. S. Black: *Modulation Theory*. (book) D. Van Nostrand Company Inc. , 1953.

[14] H. Sagan: *Introduction to the Calculus of Variations*. (book) Dover Publications Inc. New York, 1969.

[15] A.N. Kolmogorov, S.V.Fomin: *Elements of Function Theory and Functional Analysis*. MIR publisher Moscow, 1980.